Fluorometric measurements of conformational changes in glutamate transporters

H. Peter Larsson*[†], Anastassios V. Tzingounis‡, Hans P. Koch*, and Michael P. Kavanaugh†§

*Neurological Sciences Institute, Oregon Health & Science University, 505 Northwest 185th Avenue, Beaverton, OR 97006; ‡Neuroscience Graduate Program, Oregon Health & Science University, Portland, OR 97205; and §Center for Structural and Functional Neuroscience, Department of Biomedical and Pharmaceutical Sciences, University of Montana, Missoula, MN 59812

Glutamate transporters remove glutamate from the synaptic cleft to maintain efficient synaptic communication between neurons and to prevent extracellular glutamate concentrations from reaching neurotoxic levels (1). It is thought that glutamate transporters mediate glutamate transport through a reaction cycle with conformational changes between the two major access states that alternatively expose glutamate-binding sites to the extracellular or to the intracellular solution. However, there is no direct real-time evidence for the conformational changes predicted to occur during the transport cycle. In the present study, we used voltage-clamp fluorometry to measure conformational changes in the neuronal excitatory amino acid transporter (EAAT) 3 glutamate transporter covalently labeled with a fluorescent reporter group. Alterations in glutamate and cotransported ion concentrations or in the membrane voltage induced changes in the fluorescence that allowed detection of conformational rearrangements occurring during forward and reverse transport. In addition to the transition between the two major access states, our results show that there are significant Na^+-dependent conformational changes preceding glutamate binding. We furthermore show that Na^+ and H^+ are cotransported with glutamate in the forward part of the transport cycle. The data further suggest that an increase in proton concentrations slows the reverse transport of glutamate, which may play a neuro-protective role during ischemia.

G lutamate is the primary excitatory neurotransmitter in the CNS. After its release from presynaptic terminals, glutamate diffuses rapidly across the synaptic cleft and activates postsynaptic receptors. The concentration and lifetime of glutamate in the synaptic cleft are predominantly determined by the amount of glutamate released, the geometry of the synaptic cleft, and the number and localization of glutamate transporters with respect to glutamate release sites (1, 2). The activity of glutamate transporters also determines synapse independence and regulates the amount of glutamate reaching extrasynaptic receptors, i.e., glutamate spillover (2). In addition, glutamate transporters have been found to control ambient glutamate levels, thus setting the lower limit of glutamate in the brain (3, 4) and preventing glutamate from reaching neuro-toxic levels (1). Glutamate transporters possibly play a role in the progression and development of certain neurological disorders, such as amyotrophic lateral sclerosis (ALS) and epilepsy (1). Glutamate transporters have also been hypothesized to play an important role in neuronal survival during ischemia (1).

The removal of glutamate from the extracellular milieu is achieved by a family of excitatory amino acid transporters 1 to 5 (EAAT1 to -5) that are localized in glial cells and neurons (5, 6). The uptake of one glutamate molecule is coupled to the uptake of three Na^+ ions and one proton, and the extrusion of one K^+ ion (3, 7). The large electrochemical gradients for Na^+ and K^+ provide the driving force for glutamate uptake against its gradient (3). The proton has been hypothesized to play a neuro-protective role during ischemia by shutting down reverse uptake of glutamate (8), but the exact mechanism by which the proton reduces reverse transport is unclear. Although the im-portance of glutamate transporters in synaptic transmission and pathophysiology (e.g., ischemia) is well established, little is known about the molecular structure of glutamate transporters and the conformational changes that occur when glutamate is removed from the extracellular space. In addition, it is controversial as to how the different cosubstrates are coupled to the transport of glutamate (3, 9).

Several approaches have been used to probe conformational changes associated with glutamate transport. For example, Grunewald and Kanner (10) compared how trypsin cleaves the glial transporter GLT-1/EAAT2 in the presence and absence of substrates. By using antibodies raised against different parts of the transporter, they showed that trypsin cleaves the transporter into different sets of fragments when the transporter is incubated in transportable substrates (Na^+, K^+, glutamate) compared with when it is incubated in nontransportable substrates (Li^+, dihydrokinate), suggesting that the transported substrates induce conformational changes that expose additional trypsin sites. More recently, several groups have measured the accessibility of cysteine-specific reagents to cysteines introduced at different sites in glutamate transporters (11–14). By using this approach, these groups have mapped the topology of the transporters and also reported the accessibility of the studied cysteines in the absence and presence of substrates (11–15). They showed that a number of residues display substrate-dependent accessibility. However, it is unknown whether the accessibility changed as a result of a substrate-induced conformational change or whether the substrate directly protected the cysteine from the cysteine-specific reagent.

In the present work, we used voltage clamp fluorometry (VCF) to directly monitor the conformational rearrangements associated with glutamate transporters in real time (for review, see ref. 16). This technique was originally used to study conformational changes in potassium channels during the gating process (17, 18). More recently, VCF was also used in the study of glucose transporters (19, 20), γ-aminobutyric acid (GABA) transporters (21), serotonin transporters (22), and Na^+-K^+ pumps (23). VCF was developed on the finding that a fluorophore is sensitive to its local environment. Therefore, when a conformational change occurs in response to a stimulus (e.g., a change in membrane potential), the environment around the fluorophore may also change. Such an environmental change is reported as either an increase or decrease of the fluorescence signal (16). The advantage of VCF over conventional electrophysiological recording techniques (24, 25) and biochemical assays (11–14) is that VCF allows for the monitoring of real-time protein conformational changes, even if the conformational changes are electro-neutral.
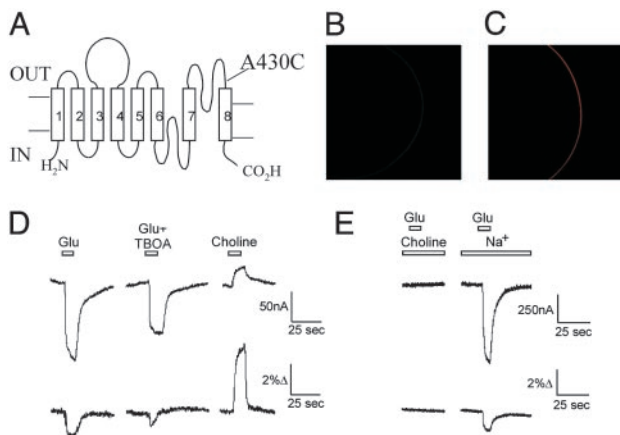
NEUROSCIENCE

Fig. 1. Fluorescent measurements report on conformational changes related to glutamate transport. (*A*) Transmembrane topology of EAAT3, showing the location of A430C that was labeled with Alexa546-maleimide. (*B* and *C*) Confocal image of the oocyte membrane, showing the fluorescence from WT EAAT3 (*B*) and A430C (*C*) transporters labeled with Alexa546-maleimide. The fluorescence measured at the membrane was >30-fold higher for 430C transporters than for WT transporters: F_{430C} = 51.4 ± 12.4 (*n* = 3) and F_{WT} = 1.7 ± 0.4 (*n* = 3). (*D*) Parallel fluorescence and current measurements of a representative oocyte during an application of 1 mM L-glutamate, 1 mM L-glutamate plus 100 μM TBOA, and 100 mM choline. V_m = −80 mV. The fluorescence baseline (before glutamate application) was >10-fold higher than the fluorescence from uninjected control oocytes. (*E*) Fluorescence and current measurements during an application of 1 mM L-glutamate in 100 mM choline or in 100 mM NaCl. V_m = −80 mV.

In this study, we detected and measured glutamate transporter-specific conformational changes by introducing a cysteine at position A430 (Fig. 1*A*) in the EAAT3 transporter (26) and subsequently labeling it with an environmentally sensitive fluorescent probe. We found that the substrates L-glutamate and D-aspartate are capable of inducing conformational changes in EAAT3. In addition, we show that there are conformational changes associated with Na$^+$ binding. Finally, we provide direct evidence that protons are cotransported with Na$^+$ through the Na$^+$-hemicycle and not, as was recently proposed, through the K$^+$-hemicycle (9).

Methods

Expression of cRNA in *Xenopus laevis* Oocytes. Cysteine mutagenesis and mRNA synthesis were performed as described. Collagenase-treated, defolliculated stage IV-V oocytes were injected with 50 ng of RNA and were incubated at 8°C in ND96 (5 mM Na/Hepes, pH 7.5/96 mM NaCl/2 mM KCl/1.8 mM CaCl$_2$/1 mM MgCl$_2$). Oocytes were incubated at 18°C for 12–15 h before experiments. Experiments were performed 3–7 days after injection.

Electrophysiology. Currents were measured at 22–25°C by two-electrode voltage clamping using a Geneclamp 500 amplifier (Axon Instruments, Foster City, CA). Data acquisition was performed with an Apple G4 computer by using a Digidata acquisition board 1322A controlled with AXOGRAPH 4.1 (Axon Instruments, Foster City, CA). Current and voltage traces were monitored with the MACLAB 2E A/D software (A. D. Instruments, Milford, MA). The currents were low-pass filtered at 1 kHz and digitized at 5 kHz. Microelectrodes were filled with 3 mM KCl (resistances of <2 MΩ), and recordings from voltage-clamped oocytes were performed with constant perfusion of Ringer's solution with various concentrations of substrates. The Ringer's solution contained 5 mM Na/Hepes, 98.5 mM NaCl, 1.8 mM

CaCl$_2$, and 1 mM MgCl$_2$ (pH 7.5). The data are reported as mean ± SE.

Labeling of Oocytes and Fluorescence Measurements. Oocytes were labeled for 60 min with 10 μM of the fluorescent maleimide probe, Alexa 546 (Molecular Probes), in Ringer's solution. Fluorescence changes were recorded under voltage clamp conditions, by using an inverted fluorescence microscope (Nikon Diaphot) with a ×20 quartz objective and a P100S photomultiplier. The objective was focused on the animal pole, and fluorescence was monitored through a rhodamine filter cube: exciter, HQ545/×30; dichroic, Q570LP; and emitter, HQ620/60m. Fluorescence signals were low-pass filtered at 200–500 Hz and digitized at 1 kHz. Fluorescence traces were monitored with the MACLAB 2E A/D software (A. D. Instruments). To control for direct effects of the different substrates on the fluorescent probe, Alexa 546-succinimyl-ester fluorophores were attached to glass coverslips coated with polylysine. The emissions from these fluorophores were measured in the same solutions that were used to study the fluorescent-labeled transporters. The change in fluorescence was very small in response to application of the different solutions. The largest change was seen when switching from a Na$^+$-containing to a choline-containing solution (<0.5%), indicating very small direct effects of the solutions on the fluorescent probes.

Modeling. Computer simulations were made with BERKELEY MADONNA (www.berkeleymadonna.com) by using a previously developed 15-state model for EAAT transporters (16, 27, 28). Fluorescence intensities were assigned to the 15 different states and fit to the steady-state fluorescence data. Several rates in an earlier model were altered to better fit the fluorescence data. The rates and the voltage dependence of the rates in the model (see Fig. 4*A*) were chosen so that two elementary charges are moved during one uptake cycle (3) and so that detail balance is maintained (29), as in the following equation: $f_1 f_2 f_3 \ldots f_{15}/b_1 b_2 b_3 \ldots b_{15} = \exp(-\Delta G_{cycle}/RT)$, where f_i and b_i are the forward and backward rates for the *i*th transition in the cycle, and ΔG is the total free-energy change during one cycle.

Results

EAAT3 Labeling and Fluorescence Measurements. We used site-directed mutagenesis to introduce a cysteine at position A430 in the neuronal glutamate transporter subtype EAAT3 (Fig. 1*A*). A430 is located in the extracellular loop between transmembrane domains VII and VIII. This region is believed to be important for glutamate binding and transport (for review, see ref. 30). After labeling with the fluorescent probe Alexa-546-maleimide, oocytes expressing A430C transporters exhibited a much higher level of fluorescence than did oocytes expressing WT EAAT3 transporters (Fig. 1 *B* and *C*). This finding demonstrates that the labeling of endogenous membrane proteins, as well as native EAAT3 cysteines, does not contribute significantly to the observed fluorescent signals. As a result, it was not necessary to use a cysteine-less EAAT3.

We established the functionality of the labeled transporter by measuring glutamate-evoked currents (Fig. 1*D*) as well as uptake of radioactively labeled glutamate (data not shown). Fig. 1*D* shows a simultaneous recording of currents and the fluorescence emission of Alexa-546-labeled A430C. The addition of 1 mM glutamate induced a current that was accompanied by a fluorescence decrease (Fig. 1*D*). The competitive transporter-blocker DL-threo-β-benzyloxyaspartate (TBOA) (31, 32) inhibited both the glutamate-activated current and the fluorescence change, suggesting that the fluorescence change was due to conformational rearrangements in the glutamate transporter (Fig. 1*D*). Fluorescence changes with the opposite polarity were seen when extracellular Na$^+$ was replaced with choline (Fig. 1*D*).
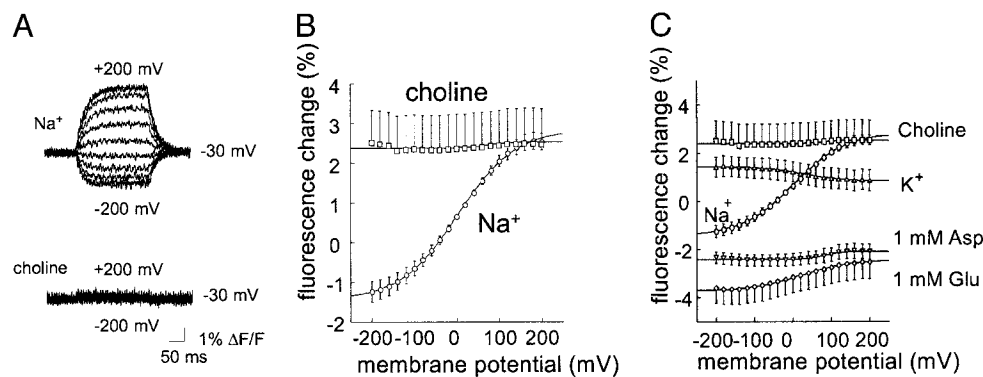
Fig. 2. Voltage- and substrate-dependence of A430C fluorescence. (*A*) Fluorescence in response to voltage steps from −200 mV to +200 mV (in increments of +20 mV), from a holding potential of −30 mV, in 100 mM Na$^+$ (upper trace) and 100 mM choline (lower trace). Each trace is the average of four identical sweeps. (*B* and *C*) Voltage-dependence of the steady-state fluorescence changes (ΔF-V) in the presence of different substrates. The fluorescence acquired at −30 mV (in 100 mM Na$^+$) was set as 0. The data were fitted to a Boltzmann function with $V_{0.5}$ = 33.1 ± 5 mV, zd = 0.34 ± .013 (n = 11) for 1 mM glutamate; $V_{0.5}$ = 75.1 ± 21.1 mV, zd = 1.3 ± .7 (n = 6) for 1 mM D-aspartate; $V_{0.5}$ = 17.9 ± 4.0, zd = 0.45 ± .04 (n = 4) for 100 mM K$^+$; and $V_{0.5}$ = −5.6 ± 2.5 mV, zd = 0.41 ± .0085 (n = 22) for 100 mM Na$^+$.

In addition, the glutamate-induced fluorescence changes were abolished when extracellular Na$^+$ was replaced with choline (Fig. 1*E*), suggesting that at least one Na$^+$ binds before glutamate. The Na$^+$ dependence and the inhibition by TBOA of the fluorescence changes indicate that the changes in the fluorescence signals are directly related to the glutamate transporter and not to other proteins endogenous to the oocytes.

Voltage Dependence of the Fluorescence Signal. To better understand the molecular mechanisms responsible for the changes in the fluorescence signals, we studied the effects of changing the membrane voltage under different ionic and substrate conditions. Previously, glutamate transporters were found to generate Na$^+$-dependent transient currents in response to changes in the membrane voltage (25, 33). These transient currents were interpreted as being due to Na$^+$ binding to sites located within the electric field where changes in membrane potential shift the distribution of transporters between the Na$^+$-unbound and Na$^+$-bound states (25, 33).

In 100 mM NaCl, the fluorescence emissions from labeled A430C increased during steps to positive voltages but decreased during steps to negative potentials (Fig. 2*A*). The steady-state fluorescence vs. voltage data were well fitted by a single Boltzmann curve with zd = 0.41 ± .0085 (n = 22) and V_{05} = −5.6 ± 2.5 mV (n = 22) (Fig. 2*B*). These values are similar to those for EAAT2, zd = 0.41 ± .07 and V_{05} = 3.2 ± 0.2 mV (n = 19), (25) and EAAT3 transient currents, zd = 0.35 ± .02 and V_{05} = −26.7 ± 0.4 mV (n = 4), suggesting that the transient currents and the fluorescence changes are due to the same process. Our data suggest that the highest fluorescence state occurs when the transporter is Na$^+$-unbound whereas the fluorescence decreases when Na$^+$ binds to the transporter. Choline cannot replace Na$^+$ as a cosubstrate for glutamate uptake (25), and, as a result, the transporter should always be in a Na$^+$-unbound state in a choline solution, regardless of the membrane potential. Consistent with this hypothesis, we found that the fluorescence in the presence of choline increased to the same level as in Na$^+$ at +200 mV where the Boltzmann function predicts 97% of transporters to be in the Na$^+$-unbound state (Fig. 2 *A* and *B*). Furthermore, we found the fluorescence in choline to be voltage-independent. In the presence of high-external K$^+$, which induces reverse transport of endogenous glutamate in the oocyte (3), we found the steady-state fluorescence vs. the voltage data to have the opposite voltage dependence from the voltage dependence in Na$^+$ (Fig. 2*C*).

The application of glutamate or aspartate decreased the fluorescence at all voltages tested, suggesting that, during trans-

port, the steady-state distribution of conformational states is shifted compared with that in Na$^+$, such that higher fluorescence states are less populated (Fig. 2*C*). In addition, the fluorescence is decreased below the fluorescence level reported in high Na$^+$ concentrations at very negative voltages, suggesting that the transportable amino acids induce a conformational change that further decreases the fluorescence (Fig. 2*C*). In the continuous presence of glutamate, the transporters will spend a large proportion of time in the state preceding the rate-limiting step in the cycle, which is believed to be the K$^+$-extrusion step (27, 28). Therefore, in the presence of glutamate, we hypothesize that the transporter will spend most of the time with its binding sites exposed to the cytosolic solution. Our results suggest that this state(s) represents a molecular conformation that is different from those with binding sites exposed to the extracellular solution and that this molecular conformation has the lowest fluorescence level.

Na$^+$ and Li$^+$ Dependence of the Fluorescence Signals. We next characterized in detail the steps preceding the binding of glutamate. Our fluorescence data are in agreement with previous work suggesting that at least one Na$^+$ binds before glutamate (25, 34). The data presented in the previous section suggest that, in the absence of glutamate, the fluorescence emission changes in parallel to the Na$^+$ occupancy of the transporter. Therefore, we measured the cation dependence of the fluorescence signal (Fig. 3*A*). In Fig. 3*B*, the voltage dependence for a steady-state fluorescence signal (ΔF-V) at different Na$^+$ concentrations is shown. Changes in the Na$^+$ concentration did not affect the slope of the curves, but rather shifted the midpoint of the curves: at higher Na$^+$ concentrations, the ΔF-V curves were shifted to depolarized potentials, and, at lower Na$^+$ concentrations, the ΔF-V curves were shifted to hyperpolarized potentials (Fig. 3*B*). These shifts of the ΔF-V curve as a function of the Na$^+$ concentration are consistent with the hypothesis that the fluorescence change monitors the Na$^+$ occupancy of the transporter. For any specific voltage, at higher Na$^+$ concentrations, more transporters will have bound Na$^+$, and, at lower Na$^+$ concentrations, fewer transporters will have bound Na$^+$.

Until recently, it was believed that only extracellular Na$^+$ ions could support amino acid transport through the EAATs, even though lithium was found to replace at least one Na$^+$ in GLT-1 (10). Borre and Kanner (35) demonstrated that, in EAAC1 (the rabbit homologue of EAAT3), L-aspartate induces steady-state currents in the presence of Li$^+$, suggesting that Li$^+$ replaces Na$^+$ at all Na$^+$-binding sites in EAAT3. They showed that Li$^+$
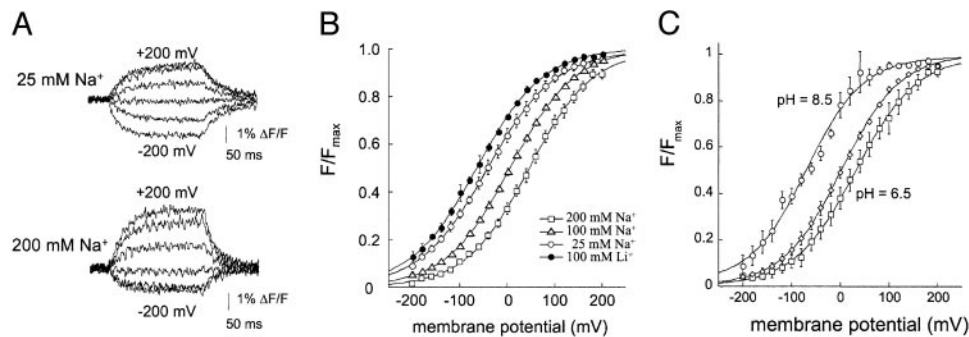
Fig. 3. Voltage dependence of fluorescence in the presence of different cation and proton concentrations. (*A*) Representative fluorescence traces from the same oocyte following voltage steps (−200 mV to +200 mV; increments of 20 mV) in the presence of 25 mM Na^+ (upper trace) or 200 mM Na^+ (lower trace), from a holding potential of −30 mV. (*B*) ΔF-V measured in the presence of extracellular Ringer's solution containing either 100 mM Li^+ ($V_{0.5} = -65.245 \pm 4.93$ mV, $zd = 0.359 \pm .014$, $n = 4$), 25 mM Na^+ ($V_{0.5} = -40.3 \pm 6.8$ mV, $zd = 0.35 \pm .023$, $n = 5$), 100 mM Na^+ ($V_{0.5} = -5.6 \pm 2.5$ mV, $zd = 0.41 \pm .0085$, $n = 22$), and 200 mM Na^+ ($V_{0.5} = 46.9 \pm 6.97$ mV, $zd = 0.376 \pm .011$, $n = 4$). To avoid any issues with osmolarity during measurements, the total cation concentration was set to a constant of 200 mM by the appropriate addition of choline. (*C*) ΔF-V measured at external pH (pH$_o$) 8.5, pH$_o$ 7.5, and pH$_o$ 6.5 in 100 mM Na^+. The data were normalized to the maximum response at each pH$_o$. The data were fitted to a Boltzmann function with $V_{0.5} = -56.4 \pm 6$ mV ($n = 11$) and $zd = 0.42 \pm 0.03$ ($n = 11$) for pH$_o$ 8.5, $V_{0.5} = -12.1 \pm 3$ mV ($n = 15$) and $zd = 0.42 \pm 0.0009$ ($n = 15$) for pH$_o$ 7.5, and $V_{0.5} = 19.2 \pm 0.01$ ($n = 10$) and $zd = 0.42 \pm 0.01$ ($n = 10$) for pH$_o$ 6.5. ΔF-V curves indicate that at −80 mV at pH$_o$ 7.5, 80% of the transporters were Na^+- and proton-bound.

supports steady-state currents, although significantly smaller in magnitude than in Na^+. To test whether Li^+ and Na^+ bind with the same affinity to EAAT3, we compared the Na^+-induced fluorescence changes to those induced by Li^+. Fig. 3*B* shows that, in the presence of Li^+, the ΔF-V curve shifts to the left without changing its slope. In particular, the ΔF-V curve in 100 mM Li^+ shifts to even more hyperpolarized voltages than the ΔF-V curve in 25 mM Na^+. This finding suggests that Li^+ binds to the same cation-binding sites and induces the same conformational changes as does Na^+, but with an ≈5- to 10-fold lower affinity.

Proton Dependence of the Fluorescence Signals. In addition to being coupled to the transmembrane movements of Na^+ and K^+, glutamate transport in EAATs is also coupled to the transmembrane movement of protons. However, it has not been resolved whether protons are transported through the Na^+-hemicycle (3, 27, 28, 36) or through the K^+-hemicycle (9). We addressed this issue by measuring the proton dependence of the fluorescence changes in the glutamate transporter. Recently, we developed a kinetic model for glutamate transporters (27, 28) and proposed that protons bind immediately before or after glutamate. In this model, or in a model where proton binding precedes glutamate binding, a change in the extracellular proton concentration should, by mass action, shift the ΔF-V similarly to a change in the extracellular Na^+ concentration. If, on the other hand, protons are either predominantly bound after glutamate (3) or in the K^+-hemicycle (9), we should observe no shift in the ΔF-V curve in the absence of extracellular K^+ and glutamate.

The steady-state fluorescence vs. voltage was measured in 100 mM NaCl at pH 6.5, 7.5, and 8.5. Changes in the concentration of pH shifted the ΔF-V curves along the voltage axis. When the proton concentration was decreased to pH 8.5, the ΔF-V curve shifted to the left. Conversely, the ΔF-V shifted to the right when the pH was lowered to 6.5 (Fig. 3*C*). The decrease or the increase in proton concentration shifted the ΔF-V curve in the same direction as did the similar changes in the Na^+ concentration, indicating that protons and Na^+ bind in the same part of the transport cycle (3, 27, 28, 36).

Discussion

In this study, we have used VCF to study conformational changes in the neuronal glutamate transporter EAAT3. The fluorescent-labeled A430C transporter displayed a decrease in fluorescence in response to the application of external glutamate. The fluo-

rescence change was partly inhibited by the transporter-blocker TBOA. The substrate-induced fluorescence changes were voltage- and Na^+-dependent. In addition, in the absence of external amino acids, the fluorescence changed in response to changes in membrane voltage. These fluorescence changes were also Na^+-dependent. The fluorescent-labeled A430C transporter used in this study was fully functional.

The fluorescence changes in response to different substrates or voltage steps imply that the transporter undergoes conformational changes, resulting in a change in the environment that the fluorophore senses. Earlier models have assumed that there are two major conformational changes that occur during glutamate transport (37): a transition of the binding sites in the glutamate-bound transporters from outside to inside, and a transition of binding sites in the K^+-bound transporters from inside to outside. However, until now, very little direct evidence for such structural rearrangements has been reported. Our data show that there are conformational changes in response to glutamate binding. In addition, our data show that an additional conformational change occurs in response to Na^+ binding because fluorescence changes are detected in response to voltage steps even in the absence of external glutamate and K^+.

To better understand the molecular mechanisms underlying these fluorescence changes, we modeled the fluorescence data by using a kinetic model (Fig. 4*A*) that we have recently developed for EAAT3 (16, 27) and EAAT2 (28), as well as for EAAT1 and EAAT4 (27). To fit the fluorescence data, we made a few minor modifications to the earlier model, which had no effect on any of our previous conclusions (27, 28). The charge valences for Na^+ and proton binding were decreased (Fig. 4*A*), and the extracellular Na^+ affinity for the first two Na^+-binding sites was altered by a factor of 2.5. We simulated the steady-state fluorescence data (Fig. 4 *B–D*) by assigning one of three fluorescence intensities to the different transporter states (where the fluorescence is given as the percentage of change from the fluorescence in our reference condition, which is defined as −30 mV in the presence of 100 mM NaCl in the absence of glutamate): T_o and T_oK each have a fluorescence value of 2.4 whereas the remaining extra- and intracellular states have values of −1.24 and −4, respectively. Three fluorescence intensity levels in a cyclic model indicated that at least three conformational changes occur during one transport cycle. The model qualitatively simulated the ΔF-V in (*i*) Na^+, K^+, choline, and glutamate (Fig. 4*B*), (*ii*) the Na^+ dependence of the ΔF-V (Fig. 4*C*), and (*iii*) the
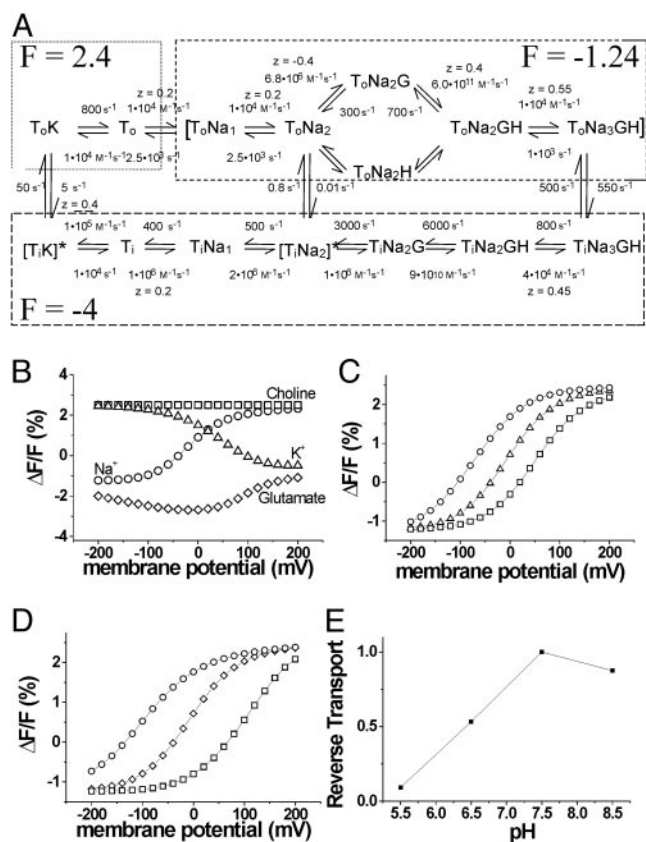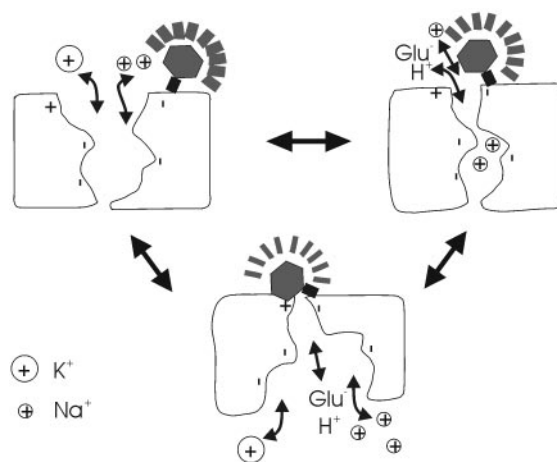
Fig. 5. Molecular model of substrate-induced conformational changes in EAAT3. Molecular schematic of the three conformational changes hypothesized in the 15-state model (Fig. 4A). A positive charge residue (marked by +) is assumed to quench the fluorescent probe attached to 430C. Na^+ binding induces a conformational change that reduces the distance between the fluorescent probe and this quenching residue. The glutamate translocation step induces an additional conformational change that further reduces the distance between the fluorescent probe and this quenching residue.

Fig. 4. An EAAT3 model with only three conformational changes simulates our experimental findings. (*A*) A modified 15-state model (16, 28) used to simulate the fluorescence data. The steady-state fluorescence data are well described by the 15-state model, after assigning three fluorescence intensities (2.4, 1.24, and −4) to the different states indicated by the dashed boxes. (*B*) Simulation of ΔF-V in different external solutions: 100 mM Na^+ (○), 100 mM choline (□), 100 mM K^+ (△), and 100 Na^+ mM plus 1 mM glutamate (◇). (*C*) Simulation of ΔF-V in different external Na^+ concentrations: 50 mM (○), 100 mM (△), 200 mM (□) (pH$_{external}$ 7.5). (*D*) Simulation of ΔF-V at different external pH: pH 6.5 (□), pH 7.5 (◇), and pH 8.5 (○); $Na^+_{external}$ = 100 mM. (*E*) Simulated reverse transport current. The steady-state reverse transport current at 0 mV is plotted at different pH (both internal and external were altered in parallel): $K^+_{internal}$ = 50 mM, $K^+_{external}$ = 50 mM, $Na^+_{internal}$ = 25 mM, $Na^+_{external}$ = 25 mM, glutamate$_{internal}$ = 10 mM, and glutamate$_{external}$ = 0.1 mM.

proton dependence of the ΔF-V (Fig. 4D). In the absence of external glutamate or K^+, the transporter is in states with binding sites exposed to the external solution: states with relatively high fluorescence in our model. The voltage dependence of the fluorescence in the absence of glutamate and K^+ is due to the voltage dependence of Na^+ binding and unbinding. The Na^+-bound states had a lower fluorescence value (ΔF = −1.24) compared with the empty transporter state (ΔF = 2.4), and, hence, the fluorescence decreased at more negative potentials. In the presence of glutamate, the transporter is mainly in states with binding sites exposed to the intracellular solution: states that have even lower fluorescence values (ΔF = −4).

In the presence of high extracellular K^+, the voltage dependence for the ΔF-V was opposite to that in the presence of extracellular Na^+. In high external K^+, EAATs have been shown to reverse direction and expel glutamate from the cell, i.e., to reverse glutamate transport (3, 38). During reverse transport, our model suggests that most transporters are accumulated on the external K^+-bound state, partly due to the slow translocation rates between T_oK and T_iK. We have previously suggested that

the transmembrane movement of ions associated with the K^+-bound transporters moves a net negative charge (27, 28). Therefore, as the membrane potential becomes more positive, the transporters most likely move to states with binding sites exposed to the intracellular solution: states that have a lower fluorescence value (−4). Therefore, the model can explain the opposite voltage-dependence of the fluorescence in high K^+ compared with Na^+ as being due to the opposite charge associated with the K^+-translocation steps compared with the Na^+-binding steps.

Our fluorescence data provide strong evidence that the transporter undergoes at least three major conformational changes during a transport cycle. In addition to the two conformational changes between the two major access states in which substrates are translocated, the data also suggest that the binding of Na^+ causes an additional conformational change because the Na^+-bound states have a much lower fluorescence than the empty transporters. We hypothesize that Na^+ binding is followed by a conformational change that occludes Na^+ within the protein (29) (Fig. 5). Such occlusion events have been observed in Na^+-K^+ ATPases (29, 39–41) and Ca^{2+} ATPases (29, 42), and they have also been suggested as a mechanism for GABA transporter-1 (GAT1) (43, 44). Also, the crystal structures of H^+-ATPase and Ca^{2+}-ATPase suggest that such occlusion and transport events require the rotational and translational movement of several helices (45, 46). For simplicity, we combined the binding and occlusion events in our model. In this model, the binding rate of a Na^+ ion, instead of being diffusion-limited ($\approx 10^8$ to $10^9\ s^{-1}$), had a significantly slower rate ($\approx 10^4\ s^{-1}$). Such a slow rate was also necessary to simulate the coupled current kinetics in outside-out patches (28), suggesting that the coupled charge movements are a combination of ion binding and occlusion events.

Although the thermodynamic coupling of protons to glutamate transport is widely accepted (3, 7), it is controversial whether glutamate is transported through the Na^+-hemicycle or the K^+-hemicycle. Zerangue and Kavanaugh (3, 36) have suggested that the proton is transported together with the Na^+ ions, based on the observation that the zwitterion L-cysteine is transported without any internal acidification, contrary to the transport of L-glutamate. Later experiments using rapid gluta-

NEUROSCIENCE

mate concentration jumps supported this hypothesis (47). In contrast, Auger and Attwell (9), studying the Purkinje neuron transporter, proposed that a proton is exchanged with a potassium ion. They based this hypothesis on their finding that changes in proton concentration did not drastically alter the kinetics of the glutamate-activated current. Our data are consistent with the first hypothesis (Fig. 3), in which the protons are transported through the Na^+-hemicycle (3, 36). In contrast, our data are not consistent with proton translocation in the K^+-hemicycle, for which changes in pH should not have any effect on the ΔF-V in the absence of K^+ and glutamate. However, our model does simulate the data of Auger and Attwell (9) (data not shown and ref. 27). We also note that, if protons bind predominantly after glutamate, there would be no shifts in the ΔF-V in response to changes in the proton concentrations in the absence of glutamate. Therefore, we conclude that, in physiological solutions and before the application of glutamate, the transporters are already in a proton-bound state. This hypothesis is consistent with our earlier model, in which the protons and glutamate bind to EAATs in random order, and the affinity of the transporters for protons is high (27, 28). Therefore, we conclude that the vast majority of the transporters are in a proton-bound state before the application of glutamate.

The question remains, however, as to why glutamate transport is coupled to the H^+ gradient. The thermodynamic value of coupling the proton to glutamate uptake is mainly due to the charge of the proton because there is only a relatively small proton gradient. We propose that the protons also have a kinetic effect rather than only a thermodynamic effect. It has been suggested that the transporters initially act as a buffer by rapidly binding glutamate, followed by a slower glutamate translocation (33, 48, 49). To buffer glutamate efficiently, the transporters must be in a state in which they can quickly bind glutamate. However, before glutamate can bind to the transporters, Na^+ ions must also bind to the transporters (25, 27, 34). At low

concentrations of protons, a large number of transporters are likely to be found in either T_o or T_oNa_1 states because the apparent affinity for Na^+ is only ≈100 mM at 0 mV (25, 34). Our model suggests that the true affinity for Na^+ is only 250 mM at 0 mV (Fig. 4A). The binding of protons after Na^+ ensures that the transporters are in a glutamate-competent state as the proton "locks" Na^+ ions into their binding sites. Hence, during physiological conditions, a majority of the transporters will be in the T_oNa_2H state, ready to bind glutamate.

Such a kinetic effect of the proton has implications during conditions such as ischemia. During ischemia, there is a collapse of ion gradients (50), and the transporters reverse to reach the new equilibrium dictated by the new ion gradients. It has been documented that the efflux of glutamate from the transporters, as they reach the new equilibrium, has detrimental effects on brain physiology (1, 51, 52). However, for transient ischemia, the speed at which the transporters reach this new equilibrium value is important. During ischemia, the extracellular and intracellular pH levels decrease to as low as 6.5 (50). As a result, the transporters are driven toward glutamate-bound states, in which case they act more like glutamate exchangers than glutamate transporters. Simulations of our model during ischemic conditions (low pH and collapsed Na^+ and K^+ gradients) show that lowering the pH slows the reverse transport significantly (Fig. 4E). The net effect is a significant slowing down of the rate at which the transporters reach the new equilibrium and, therefore, a slowing down of the rise of extracellular glutamate concentrations (8). This hypothesis suggests that the proton plays a neuro-protective role by slowing down the reverse transport of glutamate during ischemia, and thus possibly protecting neurons from excito-toxicity.

1. Danbolt, N. C. (2001) *Prog. Neurobiol.* **65,** 1–105.
2. Bergles, D. E., Diamond, J. S. & Jahr, C. E. (1999) *Curr. Opin. Neurobiol.* **9,** 293–298.
3. Zerangue, N. & Kavanaugh, M. P. (1996) *Nature* **383,** 634–637.
4. Jabaudon, D., Shimamoto, K., Yasuda-Kamatani, Y., Scanziani, M., Gahwiler, B. H. & Gerber, U. (1999) *Proc. Natl. Acad. Sci. USA* **96,** 8733–8738.
5. Rothstein, J. D., Martin, L., Levey, A. I., Dykes-Hoberg, M., Jin, L., Wu, D., Nash, N. & Kuncl, R. W. (1994) *Neuron* **13,** 713–725.
6. Chaudhry, F. A., Lehre, K. P., van Lookeren Campagne, M., Ottersen, O. P., Danbolt, N. C. & Storm-Mathisen, J. (1995) *Neuron* **15,** 711–720.
7. Levy, L. M., Warr, O. & Attwell, D. (1998) *J. Neurosci.* **18,** 9620–9628.
8. Billups, B. & Attwell, D. (1996) *Nature* **379,** 171–174.
9. Auger, C. & Attwell, D. (2000) *Neuron* **28,** 547–558.
10. Grunewald, M. & Kanner, B. (1995) *J. Biol. Chem.* **270,** 17017–17024.
11. Grunewald, M., Bendahan, A. & Kanner, B. I. (1998) *Neuron* **21,** 623–632.
12. Grunewald, M. & Kanner, B. I. (2000) *J. Biol. Chem.* **275,** 9684–9689.
13. Seal, R. P., Daniels, G. M., Wolfgang, W. J., Forte, M. A. & Amara, S. G. (1998) *Recept. Channels* **6,** 51–64.
14. Seal, R. P., Leighton, B. H. & Amara, S. G. (2000) *Neuron* **25,** 695–706.
15. Zarbiv, R., Grunewald, M., Kavanaugh, M. P. & Kanner, B. I. (1998) *J. Biol. Chem.* **273,** 14231–14237.
16. Tzingounis, A. V., Larsson, H. P. & Kavanaugh, M. P. (2002) in *Transmembrane Transporters,* ed. Quick, M. (Wiley–Liss, New York), pp. 203–215.
17. Mannuzzu, L. M., Moronne, M. M. & Isacoff, E. Y. (1996) *Science* **271,** 213–216.
18. Cha, A. & Bezanilla, F. (1997) *Neuron* **19,** 1127–1140.
19. Loo, D. D., Hirayama, B. A., Gallardo, E. M., Lam, J. T., Turk, E. & Wright, E. M. (1998) *Proc. Natl. Acad. Sci. USA* **95,** 7789–7794.
20. Meinild, A. K., Hirayama, B. A., Wright, E. M. & Loo, D. D. (2002) *Biochemistry* **41,** 1250–1258.
21. Li, M., Farley, R. A. & Lester, H. A. (2000) *J. Gen. Physiol.* **115,** 491–508.
22. Li, M. & Lester, H. A. (2002) *Biophys. J.* **83,** 206–218.
23. Geibel, S., Zimmermann, D., Zifarelli, G., Becker, A., Koenderink, J. B., Hu, Y. K., Kaplan, J. H., Friedrich, T. & Bamberg, E. (2003) *Ann. N. Y. Acad. Sci.* **986,** 31–38.
24. Wadiche, J. I., Amara, S. G. & Kavanaugh, M. P. (1995) *Neuron* **15,** 721–728.
25. Wadiche, J. I., Arriza, J. L., Amara, S. G. & Kavanaugh, M. P. (1995) *Neuron* **14,** 1019–1027.
26. Arriza, J. L., Fairman, W. A., Wadiche, J. I., Murdoch, G. H., Kavanaugh, M. P. & Amara, S. G. (1994) *J. Neurosci.* **14,** 5559–5569.
27. Tzingounis, A. V. (2002) in *Neuroscience Graduate Program* (Oregon Health & Science University, Portland, OR).
28. Bergles, D. E., Tzingounis, A. V. & Jahr, C. E. (2002) *J. Neurosci.* **22,** 10153–10162.
29. Lauger, P. (1991) *Electrogenic Ion Pumps* (Sinauer, Sunderland, MA).
30. Kanner, B. I., Kavanaugh, M. P. & Bendahan, A. (2001) *Biochem. Soc. Trans.* **29,** 707–710.
31. Shimamoto, K., Lebrun, B., Yasuda-Kamatani, Y., Sakaitani, M., Shigeri, Y., Yumoto, N. & Nakajima, T. (1998) *Mol. Pharmacol.* **53,** 195–201.
32. Shigeri, Y., Shimamoto, K., Yasuda-Kamatani, Y., Seal, R. P., Yumoto, N., Nakajima, T. & Amara, S. G. (2001) *J. Neurochem.* **79,** 297–302.
33. Wadiche, J. I. & Kavanaugh, M. P. (1998) *J. Neurosci.* **18,** 7650–7661.
34. Watzke, N., Bamberg, E. & Grewer, C. (2001) *J. Gen. Physiol.* **117,** 547–562.
35. Borre, L. & Kanner, B. I. (2001) *J. Biol. Chem.* **276,** 40396–40401.
36. Zerangue, N. & Kavanaugh, M. P. (1996) *J. Physiol.* **493,** 419–423.
37. Kavanaugh, M. P., Bendahan, A., Zerangue, N., Zhang, Y. & Kanner, B. I. (1997) *J. Biol. Chem.* **272,** 1703–1708.
38. Szatkowski, M., Barbour, B. & Attwell, D. (1990) *Nature* **348,** 443–446.
39. Holmgren, M., Wagg, J., Bezanilla, F., Rakowski, R. F., De Weer, P. & Gadsby, D. C. (2000) *Nature* **403,** 898–901.
40. Apell, H. J. & Karlish, S. J. (2001) *J. Membr. Biol.* **180,** 1–9.
41. Artigas, P. & Gadsby, D. C. (2003) *Ann. N. Y. Acad. Sci.* **986,** 116–126.
42. Toyoshima, C., Nakasako, M., Nomura, H. & Ogawa, H. (2000) *Nature* **405,** 647–655.
43. Lu, C. C. & Hilgemann, D. W. (1999) *J. Gen. Physiol.* **114,** 445–457.
44. Lu, C. C. & Hilgemann, D. W. (1999) *J. Gen. Physiol.* **114,** 429–444.
45. Kuhlbrandt, W., Zeelen, J. & Dietrich, J. (2002) *Science* **297,** 1692–1696.
46. Toyoshima, C. & Nomura, H. (2002) *Nature* **418,** 605–611.
47. Watzke, N., Rauen, T., Bamberg, E. & Grewer, C. (2000) *J. Gen. Physiol.* **116,** 609–622.
48. Diamond, J. S. & Jahr, C. E. (1997) *J. Neurosci.* **17,** 4672–4687.
49. Tong, G. & Jahr, C. E. (1994) *Neuron* **13,** 1195–1203.
50. Attwell, D., Barbour, B. & Szatkowski, M. (1993) *Neuron* **11,** 401–407.
51. Jabaudon, D., Scanziani, M., Gahwiler, B. H. & Gerber, U. (2000) *Proc. Natl. Acad. Sci. USA* **97,** 5610–5615.
52. Rossi, D. J., Oshima, T. & Attwell, D. (2000) *Nature* **403,** 316–321.